AD-A134 966 THEORETICAL MODELLING OF THREE-DIMENSIONAL VORTEX FLOWS 1/1
IN AERODYNAMICS(U) ROYAL AIRCRAFT ESTABLISHMENT
FARNBOROUGH (ENGLAND) J H SMITH JUL 83
UNCLASSIFIED RAE-TM-AERO-1963 DRIC-BR-89099 F/G 20/4 NL

END
DATE
FILMED
12 83

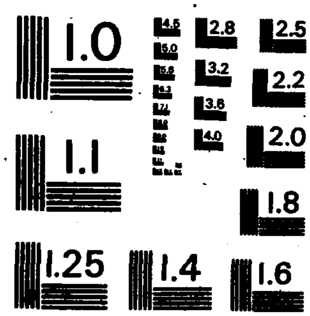

MICROCOPY RESOLUTION TEST CHART
NATIONAL BUREAU OF STANDARDS-1963-A

UNLIMITED

ROYAL AIRCRAFT ESTABLISHMENT

Technical Memorandum Aero 1963

Received for printing 8 July 1983

THEORETICAL MODELLING OF THREE-DIMENSIONAL VORTEX FLOWS IN AERODYNAMICS

by

J. H. B. Smith

Survey paper presented at AGARD Fluid Dynamics Panel Symposium "Aerodynamics of vortical type flows in three dimensions", Rotterdam, 25-28 April 1983.

LIST OF CONTENTS

SUMMARY

A unified account is presented of the various inviscid models used to represent three-dimensional vortex flows in aerodynamics; essentially those relying on vortex sheets and line-vortices. Recent developments in extending the scope, accuracy, and stability of these models are described. An evaluation of their relative strengths and weaknesses suggests that the different models all have continuing roles to play. It is claimed that vortex modelling has come of age, in the sense that we can now learn about the real world from the behaviour of models, after decades of trying to make the models conform with reality.

1 INTRODUCTION

To set the sort of model to be discussed in perspective, it is helpful to recall the usual hierarchy of flow models, together with the assumptions about the fluid and the flow which give rise to them. The first model, the Navier-Stokes equations, depends on assumptions about the nature of the fluid. Flow at large Reynolds numbers involves turbulence, and the mean motion is then modelled by the time-averaged Navier-Stokes equations, involving Reynolds stress terms. To represent these Reynolds stresses in terms of the mean motion and its history, one or more turbulence models are required. In the flow of a uniform stream past a body at a large Reynolds number, both turbulent motion and the large shears which make molecular viscosity important are confined to thin boundary layers on the body and to the wake which arises from the separation of these boundary layers from the surface of the body. Outside the boundary layers and wake the flow behaves as if the fluid were inviscid.

For most flows of importance to aerodynamics, the wakes are thin, in the sense that their thickness reduces as Reynolds number increases. The effects of turbulence and viscosity can then be modelled by the theory of thin shear layers, provided there is an appropriate model for the interaction between the external flow and the thin shear layers. A thin shear layer affects the external flow in two ways: through a displacement effect, requiring a difference in normal velocity between its opposite surfaces; and through a vortex effect, requiring a difference in tangential velocity between its opposite surfaces. As the Reynolds number tends to infinity, the displacement effect dies away, but the vortex effect remains. The shear layers become vortex sheets in the limit. This leads to an inviscid model of the flow, which is governed by the Euler equations. However, in general, the formulation of the problem for the Euler equations must include a specification of the lines on the body from which the vortex sheets arise, the separation lines.

A symmetrical wing at zero incidence sheds no vortex wake, so it is not necessary to specify a separation line. When the wing is placed at incidence the assumption that separation takes place from the sharp trailing-edge is automatically made. In reality, separation also takes place from the tip, spreading forward from the trailing-edge as the angle of incidence increases, at a rate depending on the design of the tip. For a wing with a highly-swept sharp leading-edge, a similar separation takes place from the leading edge.

We may expect that, for most bodies of practical interest to aerodynamicists, the limit of the real flow as the Reynolds number tends to infinity will be an inviscid flow with embedded vortex sheets. In this limit, it seems likely that the positions of the separation lines are determined, though not necessarily uniquely. The same flow representation may also be used as a model of the flow at large, but finite, Reynolds numbers, though then the positions of the separation lines must be supplied to the model from outside it. The assumptions leading to this model are, first, large Reynolds number and, second, the sort of thin wake flow which is naturally associated with aerodynamically efficient shapes.

For shock-free flows past bodies immersed in a uniform stream, the inviscid flow can be represented by a potential function, and the same representation can be extended to model flows with weak shock waves. From this point, at which the flow is described by a potential function everywhere outside the body and outside the vortex sheets, the various treatments to be discussed in this paper diverge. To order the discussion, we reserve the word 'model' to describe an approximation to the vortex sheet, and introduce the word 'framework' to describe a treatment of the potential flow in which the vortex sheet is embedded. Then the models of the vortex sheet to be considered are the classical rigid-wake model of a trailing vortex sheet, the Mangler-Smith model[1] for a rolled-up core, the multiple line-vortex model, and the single line-vortex model. The possible frameworks are the full nonlinear potential formulation, the nonlinear transonic small perturbation approximation, the linear small perturbation (Prandtl-Glauert) approximations for subsonic and supersonic flows, and the slender-body approximation. To illustrate the independent aspects of model and framework, a two-dimensional presentation is useful:

Framework \ Model	Rigid wake	Rolled-up core	Multiple line-vortex	Single line-vortex
Full potential	Jameson			
TSP	Albone			
P - G, M < 1	Multhopp	F.T. Johnson, *et al*[2]	Rehbach[3]	Nangia and Hancock[4]
P - G, M > 1	D. Cohen			
Slender-body	R.T. Jones	Mangler and Smith[1]	Sacks, *et al*[5]	Brown and Michael[6]

In this table the names have been introduced for illustrative purposes only. The classical rigid-wake model has, of course, been used in all the frameworks; but the other vortex models have only been used to a significant extent in the subsonic Prandtl-Glauert framework, which includes the important special case of incompressible flow, and the slender-body framework.

A further point is worth clarifying at this stage, even though it is of greater significance for Dr Hoeijmaker's paper[7]. This concerns the mathematical nature of the problems to which the various frameworks give rise, and how these can be modified by particular geometries. The discussion is restricted to steady flow. To illustrate the point, consider a purely supersonic flow and ignore the complexities of the vortex models. Both the full potential and the supersonic Prandtl-Glauert frameworks lead to hyperbolic problems. However, for the flow past a conical shape, the problem can be reformulated in conical variables, yielding an equation in only two variables which changes type from elliptic near the free-stream direction to hyperbolic at a large inclination to it. The presence of vortex sheets of conical form does not change the type of the problem in this case, though of course the presence of boundaries of unspecified shape does make it more complex. In the slender-body framework, the solution splits into an axial flow perturbation depending only on the distribution of cross-sectional area, and a cross-flow perturbation. The problem for the cross-flow is governed by Laplace's equation and is therefore always elliptic. Without the complication of the vortex sheets, each of the two-dimensional cross-flow problems is independent of the others and can be solved in isolation. With vortex sheets each cross-flow problem depends on the solution upstream. In this respect the problem takes on a quasi-parabolic character, with the streamwise coupling represented by ordinary, rather than partial, differential equations, because the circulation is concentrated in sheets, not diffused as vorticity. In the particular case of a conical body shape, for which a conical vortex configuration is sought, the quasi-parabolic behaviour is eliminated. A single elliptic problem with unknown boundaries then emerges. The other effect of introducing a vortex representation which goes beyond the rigid planar wake is to introduce an essential nonlinearity into the problem. The governing differential equations for the Prandtl-Glauert and slender-body frameworks are linear, but the condition of continuity of pressure across a vortex sheet is nonlinear.

In view of the large amount of work in this field using the slender-body framework, it is worth recalling the relationship between it and the theory of incompressible two-dimensional flow. There is an exact correspondence between the cross-flow component of a slender-body solution and an unsteady two-dimensional flow in which the body is growing, moving, and deforming in time in the same way as the cross-section of the three-dimensional body is changing in the streamwise direction. When vortex sheets are present, the separation lines must also be specified in the same way. There is no direct relationship between the viscous effects in the two- and three-dimensional flows. A consequence of this correspondence is that the classical treatment of the roll-up of a three-dimensional wake, treating it as a time-dependent problem, is just a slender-body approximation to the three-dimensional flow.

2 MODELS OF VORTEX SHEETS

The flat wake behind an elliptically-loaded wing is in equilibrium, in the classical treatment just referred to. The equilibrium is unstable, but even the existence of a simple equilibrium configuration makes this an exceptional case. In general, the equilibrium shape of a vortex sheet involves the rolling up of its free edges into a spiral form, the spiral containing an infinitely large number of turns about its axis. We shall be concerned with the representation of such spiral sheets. For a conventional, tail-aft, configuration, the rolling up of the vortex wake is of relatively little importance to the aircraft itself (though it may be very significant for a lighter, following aircraft) because it takes place well downstream of the wing and well outboard of the tail. Rolling up is of greater importance for a canard lay-out and is a dominant feature of flows involving leading-edge separation from strakes and delta wings. It is also becoming clear that the behaviour of rolled-up vortex sheets can explain many aspects of the aerodynamics of the noses of aircraft and missiles at large angles of attack.

To represent an infinite spiral in a numerical calculation would present considerable difficulties. The simplest way out is that adopted by Mangler and Smith[1]. It is simply to represent the inner turns of the vortex sheet by a single line-vortex, at least as far as the effects of the inner turns on the rest of the flow field are concerned. A few turns on the outside of the spiral can then be represented explicitly in a numerical treatment. An essential feature of flows of this kind is that circulation* is being convected along the sheet. Some simplified representation is therefore needed of the convection of circulation from the free edge of the outer part of the sheet to the line-vortex representing its core. In the existing model, used both in the slender-body and the subsonic Prandtl-Glauert frameworks, this convection process is represented as occurring entirely in the cross-flow plane, which is not very different from a plane normal to the line-vortex. As a result, a discontinuity of pressure appears across the cut connecting the free edge of the sheet to the vortex, a discontinuity whose magnitude depends on the streamwise coordinate only. To obtain a force-free system, the force which arises from this pressure difference in each cross-flow plane is balanced by the local force on the line-vortex which arises from its inclination to the local flow direction. Since the force arising from the pressure difference scales on the product of the circulation of the line-vortex and its distance from the free edge of the sheet, it will tend to zero as the extent of the properly-modelled outer part of the sheet increases. In fact, for most purposes, it is enough to include explicitly about half a turn of the sheet on a delta wing[8].

Because this model has often been applied to flows which are conical, it is often thought of as being restricted to conical flows. In fact it has been used for non-conical flows in the frameworks of slender-body theory[9,10] and of the fuller Prandtl-Glauert treatment for subsonic flow[2,11]. The boundary conditions to be applied on the properly-represented outer part of the sheet are that the pressure is continuous across the sheet and that the sheet forms part of a three-dimensional stream surface. These are exactly equivalent to the requirement that the circulation is convected with the mean of the velocity vectors on the two sides of the sheet. An additional Kutta condition is usually needed at the separation line. For flows without lateral symmetry it is also necessary to fix the overall circulation about the cross-section of the configuration to be zero; a condition which follows from the application of Kelvin's theorem to a closed contour which is convected from upstream to surround the configuration.

This model, implemented in the slender-body framework, has been shown to give a useful qualitative picture of the effects of planform, thickness, cross-sectional and lengthwise camber, side-slip, roll, and oscillations in pitch and heave for simple flows over sharp-edged wings, involving only a single pair of leading-edge vortices. It has also been implemented, with much greater difficulty, in the subsonic Prandtl-Glauert framework; and has been shown to give reliable quantitative predictions of lift, pitching moment and pressure distribution. For a discussion of these results and more complete lists of references, see previous reviews[8,12]. For these simple flows, the major weaknesses arise from the absence of any representation of secondary separation or vortex breakdown.

An important special case of this vortex-sheet model, which significantly pre-dates it, is obtained by omitting the explicit representation of the outer turns of the spiral sheet, so that the cut extends from the line-vortex to its associated separation line. This was used by Brown and Michael[6], following earlier work by Legendre[13]. The same model was applied to represent vortices shed from inclined cones and cylinders by Bryson[14], still within the framework of slender-body theory, and it has also been implemented in the subsonic Prandtl-Glauert framework[4,15]. It will be referred to as the (single) line-vortex model. Again it is not confined to conical flow, though the curvature of the line-vortex then presents a mathematical difficulty.

The self-induced velocity of a curved line-vortex is infinite and directed normal to itself. This is obviously non-physical and indicates that the model is over-simplified. The same difficulty arises with the core representation in the vortex-sheet model. It can be resolved by considering the vortex core to have a finite cross-sectional area, based on the geometry in the cross-flow plane, and a continuous distribution of vorticity, based on one of the asymptotic solutions[1,16-18] for the inner part of a vortex. The self-induced velocity is then finite, and can be calculated[19], and could, in principle, be included in the model. In the slender-body framework the self-induced velocity is of the same order as other neglected quantities and there is no mathematical reason to include it.

Another omitted effect in the representation of the whole or part of the spiral sheet by a line-vortex is that of the circumferential component of the vorticity vector. This component has the effect of accelerating the flow along the axis of the vortex, often very appreciably, producing an associated inflow as required by continuity. It is possible to represent the effect of this inflow on the outer flow by combining a line-sink with the line-vortex. This approach has been discussed by Hoeijmakers[20] and Verhaagen[21], but it is necessary to take considerable care over the definition of

---

* The term 'circulation' is here used in a slight extension of its usual meaning. Conventionally, circulation is a property of a closed contour. However, in a potential flow with embedded vortex sheets, the circulation about all closed contours which intersect one sheet only, and that sheet at one and the same point, is the same, so that it can be regarded as a local property of the sheet. It is just the jump in potential across the sheet. It seems better to extend the use of 'circulation' in this way rather than use 'vorticity' in senses which may be confusing.

entrainment if their results are to be interpreted correctly. It again appears that, in the slender-body framework, the strength of the line-sink is of the same order as the other neglected quantities.

In view of these complexities, it is not surprising that other, apparently more straightforward, approaches have been made to the modelling of the infinitely rolled-up sheet. The most popular of these is the representation of the sheet by a large number of line-vortices. The basis of this may be seen by drawing on the sheet a family of spiral curves which are lines of constant circulation, or constant jump in potential. As mentioned above, these will also be streamlines of the mean flow. The spiral curves cut the sheet into ribbons, and, if the circulation in each ribbon is condensed into a line-vortex, a multiple line-vortex model is obtained. The condition to be satisfied is simply that each line-vortex should be aligned with the local flow direction along the whole of its length.

The question of the self-induced velocity of the curved line-vortex arises again. This time the line-vortex represents, not a core of finite area, but a ribbon of the sheet, and a different approach is needed. Since a plane element of sheet has no self-induced velocity, no local contribution from the ribbon is required. A plausible procedure would be to omit from the range of Biot-Savart integral for the self-induced velocity of a line-vortex at a point P an interval surrounding P of the same length as the distance between the adjacent line-vortices. In the published calculations using this multi-vortex model, the curved line-vortices are replaced by segments of straight lines. The velocity is either calculated at the mid-point of the segment, where it is finite, or at the end, where it is presumably necessary to neglect the infinite contributions of the two segments which meet there.

The multi-vortex model is most naturally used to describe separation from the edge of a wing which is also represented by a set of line-vortices, as in a vortex-lattice or vortex-ring model of the wing. The Kutta condition is then just that the vortices run off the edge into the sheet, with continuity of circulation. If the wing is represented by a continuous load distribution, as in slender-body theory, for instance, there is some arbitrariness about where the vortices representing the sheet are to be introduced, and a similar difficulty arises in modelling separation from a smooth surface. This arbitrariness affects the circulation of the vortices through the Kutta condition.

There are three basic difficulties which affect calculations with the multi-vortex model, though the last only arises in the slender-body framework. The first is that a large number of line-vortices are needed to obtain an accurate solution. The evidence for this comes from the calculations by Sacks, *et al*[5] in the slender-body framework, where they were able to use a large number of vortices. A slight generalization of their estimate of the number of vortices needed for a converged solution is:

$$30 + 300A/\alpha \quad , \qquad (1)$$

where A is the aspect ratio and α is the angle of incidence in degrees. The largest value of A/α covered in their calculations is 0.2. There seems no reason why fewer vortices would be needed in another framework.

The second difficulty concerns the shape of the line-vortices. These should follow the streamlines and these, as we know from many visualization experiments, are helices, with the pitch of the helix becoming smaller the nearer the streamline lies to the axis of the vortex. It follows that a line-vortex starting near the apex of a delta wing should follow a helix of very small pitch, and such a helix requires very many elements to describe it with any realism. The more vortices are introduced, to meet the first difficulty, the closer to the apex the first starts, so increasing the second difficulty. The solution must be to represent the inner part of the sheet separately, probably by a line-vortex of growing circulation, as in the vortex-sheet model.

In the slender-body framework, a third difficulty arises because of the quasi-parabolic nature of the problem referred to above. The shapes of the line-vortices are found by integrating ordinary differential equations in the streamwise direction. As a result of the basic instability of this process and of the close approach of neighbouring vortices, the shapes of the vortices become chaotic, as Sacks, *et al* found[5]. This situation has since been studied in the exactly analogous planar unsteady problem, where the onset of chaos has been postponed in two ways. Moore[22] has used an explicit core representation, as suggested above for other reasons; and Fink and Soh[23] have redistributed the vortices along the sheet at the end of each time step. Recent work[24] with a multi-vortex formulation which overcomes some of these difficulties will be described later.

3 RECENT DEVELOPMENTS IN THE MODELS

Four recent developments will be outlined. Two of these relate to the adaptation of models generally applied to separation from salient edges to the representation of separation from smooth surfaces; and two arise from the need to represent more complicated flow patterns than those on a delta wing.

Let us consider first the extension of the vortex-sheet model to describe separation from smooth surfaces, as reported by Fiddes[25] for the case of the slender elliptic cone at incidence. The first point to realise is that the sheet must leave the surface tangentially[26]. There are then two possible types of behaviour of the flow normal to the separation line[26,27]. With the downstream side of the separation line defined as the side towards which the vortex sheet departs, these behaviours are: either the vortex sheet has infinite curvature and the pressure gradient upstream of the separation line is infinitely adverse; or both the sheet curvature and the upstream pressure gradient are finite. The form of the singularity in both the curvature and pressure gradient is the inverse square root of the distance from the separation line. To represent this behaviour in a calculation is not trivial, and the problem has been attempted so far only in the slender-body framework. Clearly, curved elements, or panels, are needed to represent the sheet, and the base element apparently needs infinite curvature at one end. An ingenious use of conformal mappings[25,28] avoids the need for such a special element, and an existing form[1] can be used.

From the point of view of the inviscid modelling, the outstanding question concerns the Kutta condition. Since all the velocities are finite in the attached flow, and the pressure is continuous everywhere, it is not clear that any further condition is required. However, a further condition on the numerical solution is useful. In the exact inviscid solution, the fact that both the body surface and the vortex sheet are stream surfaces implies that the velocity vector on the surface on the downstream side of the separation line must be parallel to the separation line. This will not naturally emerge from a numerical solution, in which the stream surface condition is enforced by setting the normal component of the velocity to zero. It is therefore helpful to require, as a form of Kutta condition, that the surface velocity is along the separation line on its downstream side.

From the point of view of modelling the real viscous flow, the outstanding question is the determination of the separation line. For boundary layers which are laminar upstream of separation, Fiddes describes an approach which is both rational mathematically, and reasonably successful in reproducing the observations on circular cones. The approach rests on the asymptotic theory of laminar separation for large Reynolds number which was put forward by Sychev[29] and completed by F.T. Smith[30]. The essential points are: (i) at infinite Reynolds number, separation must be smooth, *ie* the singular behaviour in sheet curvature and upstream pressure must not occur; (ii) at finite Reynolds number, the separation line is displaced downstream from the position of smooth separation until there is a balance between the strength of the singular behaviour and the level of skin friction upstream of separation.

The use of this approach, with the vortex sheet model and a laminar boundary layer calculation, makes it possible to calculate the position of the separation line as a function of Reynolds number. Fig 1 shows how the predicted movement of the separation line with Reynolds number compares with that observed by Rainbird, *et al*[31] in a water-tunnel experiment on a circular cone. The trend is well predicted, and the difference in actual position is small compared with the displacement of the separation line from its position for infinite Reynolds number. There is, of course, no reason to expect that the line along which the vortex sheet leaves the surface in the model should agree exactly with any particular observed feature of the real flow. It is surprising that the asymptotic treatment is as successful as it appears to be, relying as it does on a leading term which is of order $R^{-1/8}$.

The inviscid model can be assessed independently by using it with a measured position of the separation line. Fig 2 shows a cross-section of the calculated vortex configuration, with the separation line at the observed, laminar position; and the observed position of the core of the vortex for comparison. The vortex is at about the right distance from the surface, but not far enough round from the separation line. The same sort of discrepancy arises in wing flows, and is usually attributed to the failure to represent secondary separation in the model. A further comparison is shown in Fig 3. To give some idea of the shape of the real vortex, contours of total pressure measured by Rainbird[32] around a circular cone in a wind tunnel are shown, with the calculated vortex configuration superimposed. The observed position of the turbulent separation line was used in the calculation. The model is clearly producing the correct qualitative behaviour.

It seems perfectly feasible to extend this work to non-conical slender bodies of general cross-sectional shape, and, with rather more effort, to implement the model in the subsonic Prandtl-Glauert framework. However, to produce a similar method capable of predicting turbulent separation demands a new insight.

Compared with this substantial achievement, the second advance to be reported is a minor one. What it provides is an improvement in the Kutta condition for use with the single line-vortex model. The standard boundary condition, introduced by Bryson[14], is that the velocity at the separation line is parallel to it. This forces the separating stream surface to leave the body in a direction normal to the body, whereas, if the sheet were represented, it would leave tangentially. The improvement is achieved by writing the Kutta condition for the sheet model, that the velocity on the downstream side is parallel to the separation line, entirely in terms of the mean velocity and the rate at which circulation is being shed. These are quantities which also appear in the simpler line-vortex model and so the revised form of the Kutta condition can be taken over immediately. For the simple example of separation from a body of revolution at incidence, with the separation line lying along a meridian, the condition becomes

$$v = \sqrt{\frac{U}{2}\frac{d\Gamma}{dx}} \qquad (2)$$

where v is the circumferential component of the velocity, U is the undisturbed speed, and $d\Gamma/dx$ is the axial rate of growth of the circulation. Compared with the original form of the condition, *ie* $v = 0$, equation (2) clearly allows the vortex to be weaker if its position is unchanged. The general expression corresponding to (2) is given in Ref 12. An illustration of the effect of the different forms of Kutta condition is given in Fig 4 for conical flow. The curves drawn are all cross-sections of conical stream surfaces, of which the body surface forms one. At the top is sketched a vortex sheet solution, in which the sheet leaves the body tangentially along the separation line, S, to form the surface of separation. On the left, the flow corresponds to a line-vortex solution with the original Kutta condition: the separation line is a singular point for the family of curves shown and the separation surface leaves the body there in the normal direction. On the right, the flow corresponds to a line-vortex solution with the revised Kutta condition: the specified separation line, S, is no longer singular and the separation surface follows further round the body before leaving it, again in the normal direction. Neighbouring conical stream surfaces are now more like those in the vortex sheet solution shown at the top.

Calculations[33,34] for conical bodies using the revised Kutta condition do show smaller circulation, lower peak suction, lower lift, and vortices lying further inboard. These changes tend to improve the relationship with experimental observations. There is a lower bound on the angle of incidence for which the line-vortex model has solutions in which the vortex lies near the separation line. This bound is unrealistically high in relation to experiment and to the vortex-sheet model's predictions[25]; unfortunately the use of (2) does not lower the bound.

We now turn to the improvements aimed at the treatment of more complicated vortex configurations, in particular, configurations which involve more than one axis about which rolling-up occurs. Hoeijmakers and Vaatstra[35,36], using the vortex sheet model in time-dependent planar problems, equivalent to the slender-body framework, have introduced a very useful feature. Where, in the course of the evolution of the vortex sheet, a kink begins to form in the shape, a short segment of the sheet is removed. The circulation about this segment is concentrated into a line-vortex, which is inserted in place of the segment, and connected by cuts to the free edges of the sheet, leaving the velocity potential single-valued once more. Circulation convected off the free edges of the sheet is added to the circulation of the line-vortex. The system of a line-vortex with two cuts represents an infinitely rolled-up, double-branched core of the sheet, which we can imagine as growing from a point on the vortex sheet at which a singularity has appeared. The spontaneous emergence of singularities in the evolution of vortex sheets has recently been discussed by Moore[37] in a proper mathematical context. It appears that by identifying and treating these kinks or singularities an orderly evolution of the vortex configuration can be computed for longer times, or further downstream, than would otherwise be possible.

One of the configurations for which this sort of extra freedom is needed is the double-delta wing, or the swept-wing with strake. If the inboard and outboard portions of the leading-edge have almost the same angle of sweep and the angle of incidence is not too small, a vortex sheet will form along the whole leading-edge and roll-up into a single spiral core, just as if the planform were smoothly curved. The local disturbance to the sheet produced by the kink in the edge is quickly smoothed out. This flow should present no difficulty to any of the models.

If the kink is larger, the disturbance it causes to the smooth growth of the sheet will result in the formation of a second centre of roll-up, as sketched in Fig 5. This situation has been made visible by Verhaagen, whose photographs are published in Ref 36. The circulation shed from the outboard leading-edge cannot be convected past the newly-formed outboard core, so the circulation of the inboard part of the sheet remains constant, or may even reduce if the outboard core becomes strong enough to convect circulation back towards itself. The outboard core continues to grow on the circulation shed from the leading-edge, and will eventually dominate, and perhaps swallow, the inboard core, if the wing extends far enough. The surface sketched in Fig 5 is a stream surface, but not necessarily a proper vortex sheet everywhere. The jump in tangential velocity may decay to zero near the points of inflexion in the curves which connect the two cores, since both cores are convecting circulation away from the inflexion points.

If the kink is larger, or the incidence smaller, part of the stream surface connecting the two cores is likely to collapse onto the surface of the wing, as sketched in Fig 6. The structure of the outboard vortex is now of the familiar leading-edge vortex type, though it is worth noting that its initial growth from the kink is not conical, even in the slender-body framework. The inboard core is shown as connected to the wing surface by a stream surface springing from the line AB. This is not meant to suggest that the boundary layer on the wing separates along AB, though it might do so. However, there must be a surface streamline such as AB which forms a boundary between the surface streamlines which are swept outboard beneath the inboard core and the surface streamlines which attach to the upper surface of the wing after passing above the outboard core. Fig 7 shows a sketch of the surface streamline pattern which would be associated with the flow structure of Fig 6. AC and DE are attachment lines from which boundary layers grow. These boundary layers may collide along AB and, if they do, circulation may be shed from AB. There is some evidence[38] that this does happen on practical configurations, but interpretation of the limited experimental information is complicated by the presence of a secondary vortex formed on the forward part of the wing. For simplicity, secondary separation has been ignored in Figs 5 to 7, and the streamlines sketched in Fig 7 may be regarded either as the surface streamlines of the inviscid flow or as the limiting streamlines of the real flow.

The stream surface through AB is drawn as simply as possible in Fig 6, intersecting the wing normally. This implies that there is no shedding of circulation along AB. Part of the stream surface will then no longer be a vortex sheet, as suggested in Fig 8a. It is then likely that a second centre of roll-up will form, as in Fig 8b. On the other hand, if circulation is being shed from AB, the cross-section of the sheet will resemble Fig 8c or 8d, depending on the sign of the shed circulation. Resolving these details seems unlikely to be important.

If the flow near the kink is as sketched in Fig 6, there is still a question about its downstream development. The inboard vortex is moving slightly outboard, under the influence of its image vortex in the wing, while the outboard vortex is growing in size and strength. Will the outboard vortex capture the inboard one? We return to this question later.

As the sequence of reductions in the sweep of the outboard wing and reductions in the angle of incidence continues, the separation on the outboard leading-edge is eventually suppressed. The flow structure then resembles that of Figs 6 and 8, with the outboard vortex removed. The corresponding surface streamline pattern is sketched in Fig 9. The line AB now forms a boundary between the flow swept outboard under the vortex from the attachment line DE and the flow coming inboard from the leading-edge AC. Again there is the possibility of separation from AB and again the real flow is complicated by secondary separation on the strake. Ref 38 provides data on a flow of this kind also.

If a calculation method is to tell us which of these flow patterns actually occurs on a particular wing at a particular angle of incidence, then it must clearly be a flexible one. It may well be that Hoeijmakers technique of representing double-branched spirals provides the needed flexibility, but an alternative approach is to turn to the multiple line-vortex model.

Peace[24] has implemented a multi-vortex model, in the slender-body framework, which incorporates two improvements over the original approach of Sacks, *et al*[5]. The first of these is to allow the circulation of the vortex which was shed most recently to increase along its length. Each vortex can then start with zero circulation, at a point actually on the leading-edge of the wing; instead of starting with its ultimate strength at a point near the leading-edge. Moreover, the Kutta condition can be satisfied at every point of the leading-edge, through the continuously varying strength of the most recently shed vortex. The first vortex can be shed from the apex of a delta wing, so that near the apex the model is just the single line-vortex model. As soon as the second vortex is introduced at the leading-edge, the first vortex is no longer fed with circulation and convects with the local flow. The second vortex grows in circulation, so as to satisfy the Kutta condition; and follows a path which is determined by the condition of zero overall force on it and the cut which joins it to the leading-edge. When the third vortex is introduced, the second is shed, and so on.

The second improvement is to form a strong core vortex by successively amalgamating vortices with the first one to be shed. This is the approach successfully used by Moore[22] to delay the onset of chaos in evolutionary multi-vortex calculations. The usual technique is to replace the two vortices with one, of the same total circulation, placed at their 'centroid of circulation'. This introduces a minor discontinuity into the evolutionary process, which may trigger a potential instability. Peace avoids this by transferring the circulation, and moving the vortices, gradually, again making use of a condition of zero overall force. Two minor details of the technique are worth noting. The initial growth of each new vortex is given by an asymptotic expansion, with the numerical integration process taking over when the vortex is a short distance from the leading-edge. To avoid a multiplicity of weak vortices with a random distribution of signs being formed, vortex formation is suppressed over any length of the leading-edge for which the Kutta condition is approximately satisfied by the existing vortices. This is important in the case of a wing with lengthwise camber, to be considered later.

The new method has three significant advantages. Many vortices can be shed, to represent the flow accurately, without necessarily inducing a chaotic development. Greater smoothness in the streamwise development of the flow is achieved, though weak fluctuations remain. The overall accuracy is greater, because the flow near the apex is better represented.

Before giving an example of the capability of the method for a wing flow, we note that the technique of allowing each new vortex to grow from the separation line cannot be applied to separation from smooth surfaces. There is no asymptotic solution for the initial growth of such a vortex from a finite point, as pointed out by Bryson[14].

To illustrate the capability of this multi-vortex technique, we show the results, taken from Ref 24, of applying it to a double-delta configuration like those discussed above. The planform is defined by the equations

$$s(x) = \begin{cases} 0.1x & \text{for} \quad 0 < x < 10 \\ 1 + 0.4(x - 10) & \text{for} \quad 10 < x < 20, \end{cases} \qquad (3)$$

for the local semi-span, $s(x)$, of the wing. This corresponds to a semi-angle of 5.7° at the apex and a kink in the leading-edge of 16.1°. In Fig 10 results are shown for an angle of incidence of 5.7°. Cross-sections of the calculated vortex configuration are shown for three streamwise stations, the first at the kink. This shows the usual pattern expected of a conical vortex sheet solution for an incidence equal to the semi-apex angle. Further downstream, the vortices being shed roll-up into a new core close to the leading-edge, leaving those shed upstream to convect as a group. The last vortex shed upstream of the kink just fails to be caught up in the rotating group. The numbers beside the groups of vortices indicate the total circulation in the group, as a value of Γ/U. The value of 0.48 at the kink station compares well with that of 0.47 given by the sheet model[39] ($\Gamma/KUs = G + g = 4.7$, $K = 0.1$, $s = 1$, in the notation of Ref 39). The circulation of the outboard group grows quickly, owing to the lower sweep of the outboard leading-edge. There is no indication of any appreciable interaction between the groups of vortices at this angle of incidence.

Fig 11 shows the vortex configuration for the same cross-sections on the same planform, for an angle of incidence of 10.3°, nearly twice as large as before. Again at $x = 10$ we have the expected behaviour for a delta wing - at this incidence Ref 39 gives $\Gamma/U = 0.98$ - with a larger size and circulation corresponding to the increased incidence. Again the newly shed vortices downstream of the kink roll up in a separate group, which is also larger and stronger than before. However, at this incidence, the inboard group of vortices moves fast enough laterally, under the influence of its image in the wing, t interact significantly with the outboard group. At $x = 17.5$ the inboard group is just being broken up by the interaction. By $x = 20$, not reproduced here, the orderly struct has been disrupted, with the capture of several individual inboard vortices by the out d group. It should be pointed out that many more individual line-vortices are involved the calculation than appear in the final downstream section, because many of them have amalgamated in the cores.

4 RELATIVE ADVANTAGES OF THE DIFFERENT MODELS

As a starting point for a comparison of the advantages of the three different mo of rolled-up vortex sheets, it is helpful to describe the features which belong particularly to one of them. The remaining, shared, features are then discussed; and an overall view is formed.

The particular advantage of the single line-vortex model is its simplicity. When implemented in the slender-body framework, the model is simple enough for exact analysis to be possible. For instance, the equations governing the Bryson model[14] of separated flow over a circular cone at incidence have been reduced to a polynomial of the 18th degree, so that all solutions can be found[39]. After the obviously non-physical solutions have been rejected, a branch additional to that found by Bryson remains, and may be of physical significance. When lateral asymmetry is allowed in the Bryson model further solutions are found[40]. An asymptotic analysis of the equations is possible, for large values of the incidence parameter α/δ (best thought of as arising from small values of the cone semi-angle, δ). This confirms the physically realistic asymmetric solutions which had been found numerically; and reveals a second branch, which turns out to be non-physical.

In the case of wing problems, asymptotic expansions of the line-vortex model for small values of the circulation have proved useful. In particular they have shed light on the difficulty in finding solutions of the vortex-sheet model in two cases. The first of these is the flat-plate delta wing, for which it has proved impossible to find vortex sheet solutions which spring from the leading-edge at very small values of the incidence parameter, α/A, where A is the aspect ratio. Barsby[41] found solutions in which the sheet springs from the upper surface, just inboard of the edge. Examination of the line-vortex model shows that it, too, predicts a separation stream surface springing from the upper surface, rather than the leading-edge, when α/A is small. Asymptotic analysis shows the same situation arising on wings with non-zero thickness[42]. The second case, also discovered by Barsby[43], is of a thin delta wing with conical camber. For such a wing, the flow is attached all along the leading-edge for a particular angle of incidence, α_a. Solutions of the sheet model could be found for $\alpha < \alpha_a$, but not for a significant range of angles of incidence below α_a, for which a vortex would be expected to lie below the wing. Examination of the asymptotic expansion of the line-vortex model showed that the analytic behaviour of the solution for the cambered wing is quite different from that for the plane wing; and that no solution could be found for angles of incidence just below α_a.

The numerical work involved in applying the line-vortex model is also much lighter than it is for the vortex sheet and multi-vortex models. This would be useless unless the solutions obtained had some value. One way in which the solutions are of value is in pointing the way to existence and uniqueness properties of more complex models. Examples of this 'structural similarity' between the models, additional to those mentioned above, are given below. Levinski and Wei[44] calculated flows past cones with conical strakes in the slender-body framework and found multiple solutions for a certain range of angles of incidence. The same behaviour arises for both the line-vortex model and the vortex-sheet model, though the ranges of incidence are not the same for the two models. For a delta wing with lengthwise camber, placed at an overall angle of incidence such that the local geometric incidence falls to zero at some lengthwise station, both the vortex sheet model[9] and the line-vortex model produce unphysical results before the station of zero local incidence is reached. For laterally symmetric flow past a circular cone at incidence, there are no solutions to the line-vortex model with the vortex close to the separation line if

$$\alpha/\delta < 1.5 \operatorname{cosec} \theta_s \ , \qquad (4)$$

where θ_s is the elevation of the separation line above the horizontal*. Solutions of the vortex sheet model have been found below this limit[25], but there still appears to be a lower bound below which solutions cannot be found. When the restriction to lateral symmetry is removed, families of asymmetric solutions have been found for the line-vortex[40] and vortex-sheet[28] models. In fact, the solutions for the line-vortex model were used to find the vortex-sheet solutions.

It must be said that much of the simplicity of the line-vortex model is lost when the slender-body framework is replaced by the Prandtl-Glauert framework. Although the vortex circulation and path can still be described simply, the need to model the wake more completely than in treatments of attached flow, in order to satisfy the Kutta condition at the trailing-edge, introduces a considerable complexity[4,15]. The model has not proved popular in this framework.

The particular advantage of the multiple line-vortex model is its flexibility. In principle, circulation is shed from the separation line and convected with the local flow. In the slender-body framework, techniques following that description have been implemented and solutions, of a kind, are always obtained. The problem of the delta wing with lengthwise camber mentioned above illustrates this advantage of the multi-vortex model very clearly. Both the vortex-sheet model and the single line-vortex model break down because they are not sufficiently flexible to represent the change from shedding circulation towards the upper surface over the forward part to shedding it towards the lower surface over the rearward part. Peace[24] has treated the problem using his multi-vortex model to obtain the results shown in Fig 12. The planform of the wing is defined by the local semi-span

$$s(x) = 0.25x \quad . \tag{4a}$$

The apex region of the wing is at a uniform positive incidence, given by

$$\frac{\partial z}{\partial x} = -0.2 \qquad \text{for} \quad 0 < x < 1. \tag{4b}$$

Further aft, the local incidence reduces smoothly, passing through zero at $x = 2$, after which it is negative:

$$\frac{\partial z}{\partial x} = -0.2(2-x) \qquad \text{for} \quad x > 1. \tag{4c}$$

Fig 12 shows sections through the vortex configuration for four stations, all downstream of the conical flow region. Note that only the region near the leading-edge is illustrated at each station. At $x = 1.4$, the multi-vortex configuration, shown by the circles, agrees quite well with Clark's sheet solution[9], shown by the line and cross. By $x = 1.8$ no further positive vortices have been shed, as indicated by the unchanged figure for the circulation above the wing, but a single negative vortex, represented by a solid circle, has just been shed towards the lower surface. The geometric incidence is still positive at this station. Clark's solution also shows negative circulation being shed, but the shape of the sheet has begun to look unrealistic, and the solution could not be extended further downstream. The multi-vortex solution will go further: by $x = 2.2$ a rolled-up system of negative vortices has formed below the wing, though its strength is still weak compared with the upper surface vortex, now reduced to a core by the operation of the amalgamation algorithm. By $x = 2.6$, the negative system is stronger than the positive one. Note how the interaction between the systems has drawn both of them outboard of the leading-edge. Not surprisingly, the orderly structure is disrupted in a relatively short further distance downstream, before the local incidence reaches a negative value as large as the positive value at the apex.

Further evidence of the flexibility of the multi-vortex method is provided by the calculations for the double-delta wing shown in Figs 10 and 11 and discussed above. Many calculations of time-dependent planar flows and of the evolution of trailing vortex wakes show the same flexibility. Hoeijmaker's recent work[35,36] has made the vortex-sheet model more flexible, while Peace's use of an amalgamation algorithm has made the multi-vortex model rather less flexible. The two models are perhaps moving towards a common capability, but the multi-vortex model is still the more flexible.

When the multi-vortex model is implemented in the Prandtl-Glauert framework for steady, subsonic flow, the problem becomes elliptic. The simple idea of shedding and convecting circulation no longer applies, since what is shed downstream affects the flow upstream. Considerable ingenuity may then be needed to obtain solutions for flows with a simple structure, as Rehbach[45] and Schröder[46] found for the case of the delta wing. The difficulty is presumably that the flexibility of the model is not yet matched by a corresponding flexibility in the numerical schemes available to solve the large number of nonlinear simultaneous equations to which the model gives rise. It would seem worth trying to exploit the existence of slender-body techniques: either to provide an initial guess for the Newton-Raphson method, as Forrester, *et al*[2] do; or as a step in an iterative method, as Jepps[47] has proposed.

For unsteady incompressible flow, the problem is again an evolutionary one and the flexibility of the multi-vortex model reappears[48,49,50]. Unfortunately, the tendency for the motion of the vortices to become chaotic also reappears. It seems that neither steady nor truly periodic solutions have been produced as a result of evolutionary calculations, and, in their absence, it is hard to assess the accuracy of the calculations.

* NB this is a different definition of θ_s from that in Fig 1.

The particular advantage of the vortex-sheet model lies in the greater realism with which it describes separation from a line on a smooth surface. As indicated earlier, the theory used by Fiddes[25] to calculate the position of laminar separation on a cone requires the strength of the singular behaviour of the inviscid solution at the separation line. This can only be found from a vortex-sheet model. Even if it is not intended to predict the position of the separation line, it still seems unlikely that reasonable accuracy can be obtained without treating the inviscid flow near the separation line adequately. The sketches of Fig 4 show the sort of qualitative difference that can arise. As an extreme example of the quantitative differences between the predictions of the vortex-sheet model and the predictions of the single line-vortex model, we have Fig 18, which is discussed in detail later. The discrepancy is far greater than that for flows over wings.

The common advantage of the vortex-sheet and multi-vortex models over the line-vortex model is that they both offer a closer approximation to the infinite Reynolds number limit of the real flow. As would be expected, they almost always give closer agreement with measurements at finite Reynolds number. As between these two models, the remaining advantages are less clear cut. In the terminology of panel methods, the sheet model is a higher-order method. Consequently it gives greater accuracy for a similar number of elements, with the ability to predict a smooth behaviour of the flow. On the other hand, the programming effort involved in the sheet method is greater, and computing time for the same member of elements should also be greater. At present no comparison can be made on the basis of computing time for the same accuracy, but the multi-vortex method must involve more storage space. If it is desired for some reason to represent many turns of a rolled-up configuration, the vortex-sheet model has an advantage, because a multi-vortex calculation is likely to be disrupted by vortices from adjacent turns pairing-off and rotating round one another.

A large potential advantage of a multi-vortex model in the subsonic Prandtl-Glauert framework is that it might well predict vortex breakdown. In fact Aparimov, *et al*[51] claim that the failure of their multi-vortex model to converge at a large angle of incidence is related to vortex breakdown in the real flow. Rehbach, aiming particularly at the calculation of unsteady incompressible flow, has introduced[52] a Lagrangian model based on the vorticity equation, which has some resemblance to a multi-vortex model. The outcome is a set of streak-lines which spring from the separation line, in a direct simulation of Werlé's famous dye-lines. Rehbach also claims[53] that the disorganization of the calculated streak-lines near the axis of the vortex corresponds to vortex breakdown. It should also be possible to predict at least the initial occurrence of vortex breakdown using the vortex-sheet model in combination with a technique like that of Hall[54] for calculating the flow in an axisymmetric core of distributed vorticity. By averaging the predictions of the vortex-sheet model in the circumferential direction, the inward flow of mass and circulation to the core and the pressure distribution along it could be obtained. These are the boundary conditions required for the core calculation, which would in turn supply a displacement effect along the axis of the vortex in the sheet model. So far as the prediction of breakdown is concerned, it cannot be said that either model has the demonstrated capability, nor that either is incapable. It may well be that a direct attack on the Euler equations, like the one Rizzi describes[55], will provide the best approach to the problem.

In summary, if a method of useful accuracy is required, the choice is between the vortex-sheet and multi-vortex models. For separation from smooth surfaces, the sheet model is preferable. If the same program is required to calculate very different vortex structures with minimal changes, the multi-vortex model is preferable. The line-vortex model has a useful role to play in initial investigations and in suggesting the underlying structure of families of solutions of the more realistic models.

5 WHY MODELLING?

Since these models all lead to such complexities and still fall short of a proper description of the behaviour of the fluid, we must ask whether it is worthwhile pursuing them further. After all, solutions of the Navier-Stokes equations and the Euler equations by field methods are becoming available and must eventually become the accepted methods for making quantitative predictions about vortex flows. Nonetheless, I believe it is worth continuing with modelling techniques. In support of this view, I have first some very general remarks, which can conveniently be put as quotations, and then an account of how modelling has recently helped with a particularly intractable problem.

To start with, here is a quotation from a lecture[56] given by James Lighthill to the Royal Aeronautical Society, when he was Director of the RAE. He is speaking of the role of mathematics in generating physical ideas.

"Examples of this mathematically generated kind of physical idea, which I have already mentioned, are trailing vorticity, boundary layer, dynamic stability and Nyquist diagram.

The value of physical ideas in practical work, of course, is their elasticity. Provided that they are sound ideas, such as those thrown up as the genuinely appropriate physical description of the mathematical solution of some well defined class of problem, they usually show a splendid capacity to stand up to distortions of the problem, and indeed to radical changes and complications in its conditions, and still give the right guidance about what needs to be done. In other words, a well designed physical idea has wide elastic limits, and will tolerate being pulled and twisted about, and go on giving good service in suggesting the right experiment, or the way out of such and such a difficulty, or in giving someone a feeling tha ... is not just dismally accumulating a confused mass of experimental data, but there is some thread running through them which gives them meaning and interest. Naturally, then, these ideas are much in demand, and when we come to a new kind of problem, where we are short of physical ideas because none of the old ones that we are accustomed to seems to give any help in solving it, then we can only hope that someone will come along with a mathematical treatment of some appropriately simplified, although possibly also generalised case, and interpret its solution by introducing a new animal into the zoo of useful aeronautical concepts, preferably a well-behaved beast, which all of us will in due course be able to ride as to the manner born, probably ignoring, if we are not mathematicians, what kinds of technique were used to lick him into shape."

Lighthill went on to discuss the role of mathematics in getting actual answers.

Now for a quotation from the final section of Dietrich Küchemann's book[57] on the aerodynamic design of aircraft.

"Above all, it is such conceptual frameworks which enable us to formulate intelligent ways of modifying and controlling our part of human endeavours. Ideas and concepts come out of the mind, not out of computers or wind tunnels. If there is one overriding purpose throughout these notes, above all others, it is to demonstrate the continued need for conceptual frameworks and for understanding the physics of airflows in any work on aerodynamic design."

Finally, because I have not found a better way to express the idea since, a quotation from a previous AGARD paper[58] of my own.

"The philosophical argument naturally concerns ends rather than means. If our aim is to reproduce our bit of the real world in a computer, then the solution of the Navier-Stokes equations is a possible approach, at least for laminar flows. We may hope to obtain more precise information, more quickly and more cheaply than by making measurements in real fluids, and this is well worth doing. However, as scientists we wish to understand things, and as engineers we wish to alter things. In both of these processes the acquisition of data needs to be accompanied by the growth of conceptual frameworks which can account for the data we already have and show us where more is needed. It is such conceptual frameworks which enable us to formulate intelligent ways of modifying and controlling our bit of the universe. They are built of models, some far-reaching and all-embracing, but some quite special. I do not see the need for special models disappearing in our field. In particular, I expect the distinction between the external inviscid flow and the boundary layer, on which the science of aerodynamics has been built, to continue, supplemented locally by special models of separation phenomena."

These quotations put the abstract case for modelling very clearly, but they do not provide much in the way of illustration. It is therefore appropriate to turn to a description of some recent work with two of the models that have formed the basic theme of this paper, work that has significantly increased our understanding of some baffling observations. These observations are of the lack of expected symmetry in flows past bodies at large angles of incidence, leading to very significant out-of-plane forces on missiles and to large yawing moments on aircraft[59]. The work is that described by Fiddes[28] at the Trondheim meeting last year, using first the line-vortex model and then the vortex-sheet model, and in each case showing the existence of a second family of solutions which produce large out-of-plane forces on circular cones. I shall conclude by suggesting that the simplifications implicit in the models have actually helped to bring about the increased understanding.

Both models are implemented in the framework of slender-body theory and applied to flow past circular cones at incidence. The line-vortex model is then simply the one which was devised by Bryson[14]; the only change is that the port and starboard vortices are allowed to lie asymmetrically about the incidence plane and to have different circulations, and that the separation lines are also allowed to be asymmetrically placed. The model is entirely inviscid, so the positions of the separation lines must be supplied to it. The separation lines are supposed to be generators of the cone. The entire geometry is then conical, so, since slender-body theory is used, the existence of a conical flow solution is to be expected. This means that the solution sought depends on three parameters: the angular positions of the two separation lines round the circumference of the cone, and an incidence parameter, α/δ , which is the ratio of the angle of incidence, α , to the semi-apex angle of the cone, δ . The entire flow field can be written down in terms of these three parameters and six unknown quantities: the two coordinates and the circulation of each of the two vortices. Six conditions are available to determine these six unknowns: a Kutta condition at each separation line, and the vanishing of the two cross-flow components of the overall force on the combination of each vortex and the cut which joins it to the appropriate separation line. The original form of the Kutta condition is retained.

The equations expressing the two Kutta conditions are linear in the two circulations and so can be solved for them. The expressions which result can be substituted into the remaining four equations, which are then extremely nonlinear in the four coordinates of the vortices. A generalized Newton-Raphson technique is used to solve these equations. The results are most easily understood by concentrating on the case in which the two separation lines are placed symmetrically with respect to the incidence plane, so that the solutions depend only on the separation line position and the incidence parameter. Fig 13a&b shows the variation of the two coordinates of the starboard vortex, as the incidence parameter increases, for separation lines which are $\theta_s = 56°$ round from the 'horizontal' plane through the axis of the cone. The coordinates are referred to horizontal and vertical axes in the cross-flow plane, with origin on the cone axis. For small values of the incidence parameter, no solutions have been found. For values above the limit of 1.81, given by equation (4), Bryson's symmetric solutions appear. No others have been found until the point B on the symmetric solution curve is reached. Here the solution, as a function of α/δ, bifurcates in the classical manner, with the Jacobian matrix becoming singular. Two further solution branches exist for larger values of α/δ and these are mirror images in the incidence plane. It is only the intersection at B in Fig 13 which represents a bifurcation; at the other intersections only one of the two coordinates agrees.

It is easier to appreciate the solutions when the loci of the vortices are plotted in the cross-flow plane for varying values of the incidence parameter. Fig 14 shows the symmetric solution and one of the asymmetric solutions for values of α/δ between 3 and 10, and a rather earlier separation position, $\theta_s = 40°$. It is necessary to check that the flow on the surface of the cone does actually converge towards the postulated separation lines, since the equations are equally well satisfied by attaching flows. It turns out that the solutions are physically sensible for values of α/δ up to a value rather greater than the largest in Fig 14. Since the slender-body framework assumes the incidence is small, such large values of α/δ would be irrelevant for practical configurations.

Fig 15 shows the asymmetry in the circulation of the vortices, the strength of each being referred to the strength of the vortices in the symmetric solution for the same value of α/δ. The range of values of α/δ does not extend downward as far as the bifurcation point, so the curves do not start with a common value of unity, as they should. In view of the very different loci shown in Fig 14, it is somewhat surprising that the circulations of the asymmetric vortices are not more different from one another and from those of the symmetric vortices. It is well known that slender-body theory tends to overpredict lifting forces and the line-vortex model also tends to overpredict the nonlinear contributions. Therefore, to make a comparison with force measurements, the ratio, C_Y/C_N, of side force to normal force is presented in Fig 16. The separation lines are still symmetrically placed at the arbitrarily selected value, $\theta_s = 40°$. The theoretical curve needs no explanation, since it arises directly from the asymmetric solutions described. The experimental points are taken from the measurements by Keener, *et al*[60]. Each point represents the largest value of C_Y/C_N measured at that particular angle of incidence, so the roll angle and Reynolds number may be different for the different points. The agreement with observation is striking in view of the simplicity of the model and the framework.

It is clear that asymmetric effects comparable with those observed can be produced by an entirely inviscid mechanism, separation having been fixed symmetrically in the calculations. To make it clear that this mechanism is the relevant one, a further step is needed. As explained above, the model allows the positions of the separation lines to be chosen freely, but so far the results presented have been for separation lines placed symmetrically about the incidence plane. Solutions for asymmetrically placed separation lines can be obtained by proceeding in small steps from either a symmetric solution or an asymmetric solution with symmetric separation lines. Obviously all the solutions obtained in this way are asymmetric, but they fall into two distinct families: the first family derives from solutions which are symmetric when the separation lines are symmetric; the second derives from solutions which are asymmetric when the separation lines are symmetric. The importance of the second family can be confirmed by examining the level of side force produced by the first family. Fig 17 shows typical values of the ratio of side force to normal force that correspond to solutions of the first family, for an incidence parameter of 3.5. For this value of the incidence parameter, Fig 16 shows the experimental value is 0.75, so the calculated values in Fig 17 are smaller by an order of magnitude. The abscissa in the figure is the degree of asymmetry in separation line position, and the curves are drawn for fixed positions of one of the separation lines. It is concluded that the second, globally asymmetric, family of solutions is needed to produce the observed results on cones, and that it is capable of generating side forces of the right order.

The vortex-sheet model has subsequently been applied to the same configuration, in the same framework. This offers two advantages: an increase in accuracy, and the possibility of extending the calculation to the prediction of laminar separation, as previously demonstrated[25] for the symmetrical case. So far, however, the vortex-sheet model has been used with specified separation lines, in the same way as the line-vortex model. The asymmetric solutions of the line-vortex model were only found after a long search, but it was hoped that they would provide a good starting point from which to seek solutions of the vortex-sheet model. In fact, the search for sheet solutions took even longer.

Fig 18 shows one of those found, with, on the left, the symmetric solutions for the same incidence parameter and separation line position. For comparison, the positions of the line-vortices in the corresponding solutions for the simpler model are shown by solid circles. For the symmetric solutions on the left, the difference between the core positions for the two models is not much greater than that familiar from solutions for delta wings, and of a similar form. However, the asymmetric solutions on the right seem scarcely related. This may be a rather extreme example - the starboard line-vortex has moved initially downwards and outboard from the bifurcation point - but the differences between the asymmetric vortex positions predicted by the two models are generally large. This explains why it was hard to find the vortex-sheet solutions, but indicates that the effort was probably worthwhile. The starboard sheet in the asymmetric solution is very similar in appearance, and, in turns out, in structure, to the symmetric sheets; but the port sheet is quite different. In shape it is like the conical trailing vortex sheet calculated by Jones[61], and its structure is also similar in that only a small part of the total circulation lies in the core, with the bulk of it on the sheet. Fig 19 shows a vapour-screen photograph due to Peake, *et al*[62] of the flow over a circular cone at a similar value of the incidence parameter, in which the vortices are visible as dark regions. There is clearly a remarkable resemblance between the calculated solution and the visualisation of the flow.

Ref 28 also includes a comparison of the forces predicted by the vortex-sheet model with those measured in some unpublished work by Mundell at RAE. The positions of the straight, laminar separation lines were measured along with the forces, with the flow tripped at the apex by a tiny protuberance. Great care was taken to ensure that measured forces arose from a region of approximately conical flow. The live portion of the model is a circular cone of 10° semi-apex-angle, with a length of 292 mm. Forces were measured over a range of Reynolds numbers in a low-speed wind tunnel, for a continuously-varying roll angle. The values chosen for comparison correspond to the largest Reynolds number for which the boundary layer at separation is wholly laminar, and to the roll angle for which the side force is greatest. At an angle of incidence of 36°, the observed separation lines lay in the 'horizontal' reference plane on one side and 14° above it on the other side. (It is worth noting in passing that this degree of asymmetry in the separation line position is small compared with the range considered in Fig 17.) Any calculated solution with these separation lines must be asymmetric; but there is again a distinction between a first family of solutions which derive from a symmetric solution and a second family whose members derive from solutions which are asymmetric even when their separation lines are symmetric. The solutions from the first and second families, for the experimental value of the incidence parameter and measured separation positions, are illustrated in Fig 20. The table below shows some details of these solutions and a comparison of the forces.

		First family	Second family	Experiment
Total circulation	left	-13.7	-13.9	
	right	16.0	14.0	
Core circulation / Total circulation	left	0.64	0.80	
	right	0.60	0.25	
C_Y/δ^2		-1.5	-19.7	-17.6
C_N/δ^2		36.8	36.8	27.0

The table shows first that the circulations of all the vortices are similar, despite the very different shapes of those in the second family solution. However, the different shapes are accompanied by a difference of structure: most of the left-hand vortex circulation is in its core, and most of the right-hand vortex circulation is on the sheet. The force coefficients are based on the plan area of the cone; each is divided by δ^2 to bring it to a similarity form. The side force in the first family is smaller than that measured by an order of magnitude, but the second family prediction is close, considering it is based on slender-body theory. The normal force is almost the same for the two solutions and much larger than the measurement. The discrepancy is not surprising, since the slender-body framework relies on the angle of incidence, 36° in the experiment, being small. There can be little doubt that the solution from the second family corresponds to the experimental situation.

The success of this work in explaining the origin of the large side forces measured on circular cones at angles of incidence greater than the apex angle is very significant, but it is only the first step in the process of explaining the observations of side force on practical aircraft and missile shapes. For instance, in a conical flow the local side force coefficient is the same along the whole length of the cone, whereas the oscillatory variation of the local side force along the length of an ogive-cylinder is well known. Moreover, a significant level of side force arises on an ogive-cylinder at angles of incidence too small in relation to its apex angle for the second family of solutions to exist at the apex. However, the work has identified one mechanism which must exert an important influence on the aerodynamics of slender pointed bodies. Before it there was only conjecture about the origin of out-of-plane force. After it, one origin is clear.

I think this is the first time that vortex modelling, in the sense used in this paper, has actually told us something we did not know before. After decades of trailing behind experimental observation and measurement, models have at least repaid our efforts by telling us something about the real world.

Obviously we should be trying to overcome the limitations of models, and much of this paper has been devoted to efforts to do so. However, there is a sense in which the very limitations of the models used can contribute to the clarity of the outcome. It is the need to supply the separation lines to the inviscid model which forces the isolation of the large-scale asymmetry of the second family from the small-scale asymmetry of the first family. It is the consideration of conical flow which concentrates attention on the flow at the apex of the body. It is the use of the simplest possible model which reduces the behaviour of the solution from being that of a three-dimensional continuum, as is the case when the steady Euler or Navier-Stokes equations are solved, to a dependence on four numbers, the coordinates of the line-vortices; and so makes it possible to contemplate a systematic search for solutions.

It is too much to hope that second family solutions, even with a more appealing name, will ever come to figure alongside 'boundary layer' and 'trailing vortex' in a list of concepts given by mathematics to aeronautics, but they do encourage us to keep modelling.

REFERENCES

1 K.W. Mangler, J.H.B. Smith: "A theory of the flow past a slender delta wing with leading-edge separation." Proc. Roy. Soc. Lond. A, 251, 200-17 (1959); also Report Aero 2593 (1957)

2 F.T. Johnson, P. Lu, E.N. Tinoco, M.A. Epton: "An improved panel method for the solution of three-dimensional vortex flows: Vol.1 - Theory document." NASA CR-3278 (1980)

3 C. Rehbach: "Numerical investigation of leading-edge vortex for low aspect ratio thin wings." AIAA J, 14, 253-5 (1976)

4 R.K. Nangia, G.J. Hancock: "A theoretical investigation for delta wings with leading-edge separation at low speeds." ARC CP 1086 (1968)

5 A.H. Sacks, R.E. Lundberg, C.W. Hanson: "A theoretical investigation of the aerodynamics of slender wing-body combinations exhibiting leading-edge separation." NASA CR-719 (1967)

6 C.E. Brown, W.H. Michael: "Effect of leading-edge separation on the lift of a delta wing." J. Aero. Sci. 21, 690-4 and 706 (1954)

7 H.W.M. Hoeijmakers: "Computational vortex flow aerodynamics." In AGARD FDP Symposium 'Aerodynamics of vortical type flow in three dimensions' (1983)

8 J.H.B. Smith: "Achievements and problems in modelling highly-swept flow separations." In 'Numerical methods in aeronautical fluid dynamics' (ed. P.L. Roe), Academic Press (1982)

9 R.W. Clark: "Non-conical flow past slender wings with leading-edge vortex sheets." ARC R & M 3814 (1976)

10 I.P. Jones: "Leading-edge separation from a slender rolling wing-body combination." RAE Technical Report 80039 (1980)

11 E.N. Tinoco, P. Lu, F.T. Johnson: "An improved panel method for the solution of three-dimensional vortex flows: Vol.2 - Users' guide." NASA CR-3279 (1980)

12 J.H.B. Smith: In 'Three-dimensional and unsteady separation at high Reynolds numbers', AGARD-LS-94 (1978)

13 R. Legendre: "Écoulement au voisinage de la pointe avant d'une aile à forte flèche aux incidences moyennes." Rech. Aero. Nos.30, 31 and 35 (1953)

14 A.E. Bryson: "Symmetrical vortex formation on circular cylinders and cones." J. Appl. Mech. (ASME), 26, 643-8 (1959)

15 T.K. Matoi, E.E. Covert, S.E. Widnall: "A three-dimensional lifting-surface theory with leading-edge vortices." US Office of Naval Research ONR-CR-215-230-2 (1975)

16 M.G. Hall: "A theory for the core of a leading-edge vortex." J. Fluid Mech. 11, 209-28 (1961)

17 S.N. Brown: "The compressible inviscid leading-edge vortex." J. Fluid. Mech. 22, 17-32 (1965)

18 K.W. Mangler, J. Weber: "The flow field near the centre of a rolled-up vortex sheet." J. Fluid Mech. 30, 177-96 (1967)

19 D.W. Moore, P.G. Saffman: "The motion of a vortex filament with axial flow." Phil. Trans. Roy. Soc. Lond. A, 272, 403-29 (1972)

20 H.W.M. Hoeijmakers, W. Vaatstra: "A higher-order panel method for the computation of the flow about slender delta wings with leading-edge vortex separation." NLR MP 81053U (1981)

21 N.G. Verhaagen, L. van der Snoek: "An experimental investigation into the entrainment into a leading-edge vortex." Delft Univ. of Techn. Report LR-332 (1981)

22 D.W. Moore: "A numerical study of the roll-up of a finite vortex sheet." J. Fluid Mech. 63, 225-35 (1974)

23 P.T. Fink, W.K. Soh: "A new approach to roll-up calculations of vortex sheets." Proc. Roy. Soc. Lond. A, 362, 195-209 (1978)

24 A.J. Peace: "A multi-vortex model of leading-edge vortex flows." To appear in Int. J. of Numerical Methods in Fluids (1983)

25 S.P. Fiddes: "A theory of the separated flow past a slender elliptic cone at incidence." Paper 3C in 'Computation of viscous-inviscid interactions', AGARD CP 291 (1980)

26 J.H.B. Smith: "Behaviour of a vortex sheet separating from a smooth surface." RAE Technical Report 77058 (1977)

27 F.T. Smith: "Three-dimensional viscous and inviscid separation of a vortex sheet from a smooth non-slender body." RAE Technical Report 78095 (1978)

28 S.P. Fiddes, J.H.B. Smith: "Calculations of asymmetric separated flow past circular cones at large angles of incidence." Paper 14 in 'Missile aerodynamics', AGARD CP 336 (1982)

29 V.V. Sychev: "On laminar separation." Izv. Ak. Nauk Mekh. Zh. Gaza, No.3, 47-59 (1972); Trans. in Fluid Dynamics, Plenum, March 1974, 407-417

30 F.T. Smith: "The laminar separation of an incompressible fluid streaming past a smooth surface." Proc. Roy. Soc. Lond. A, 356, 443-63 (1977)

31 W.J. Rainbird, R.S. Crabbe, L.S. Jurewicz: "A water-tunnel investigation of flow separation about circular cones at incidence." NRC (Canada) Aeron. Rep. LR 385 (1963)

32 W.J. Rainbird: "The external flow field about yawed circular cones." Paper 19 in AGARD CP 30 (1968)

33 R.K. Nangia: "A study of slender conical thick wings and bodies with variation of flow separation point." Bristol Univ., Dept of Aero. Eng., Grant No.AFOSR-77-3243 (1978)

34 K. Moore: "Line-vortex models of separated flow past a circular cone at incidence." RAE Technical Memorandum Aero 1917 (1981)

35 H.W.M. Hoeijmakers, W. Vaatstra: "A higher-order panel method applied to vortex sheet roll up." AIAA Paper 82-0096 (1982)

36 H.W.M. Hoeijmakers, W. Vaatstra: "On the vortex flow over delta and double-delta wings." AIAA Paper 82-0949 (1982)

37 D.W. Moore: "The spontaneous appearance of a singularity in the shape of an evolving vortex sheet." Proc. Roy. Soc. Lond. A, 365, 105-19 (1979)

38 P.J. Butterworth: "Flow measurements in the wake of a wing fitted with a leading-edge root extension (strake)." RAE Technical Report 79120 (1979)

39 J.H.B. Smith: "Improved calculations of leading-edge separation from slender, thin, delta wings." Proc. Roy. Soc. Lond. A, 306, 67-90 (1968); RAE Technical Report 66070 (1966)

40 D.E. Dyer, S.P. Fiddes, J.H.B. Smith: "Asymmetric vortex formation from cones at incidence - a simple inviscid model." Aeronautical Quarterly 33, 293-312, November 1982; also RAE Technical Report 81130 (1981)

41 J.E. Barsby: "Separated flow past a slender delta wing at low incidence." Aeronautical Quarterly 24, 120-8 (1973)

42 R.W. Clark, J.H.B. Smith, C.W. Thompson: "Some series-expansion solutions for slender wings with leading-edge separation." ARC R & M 3785 (1975)

43 J.E. Barsby: "Flow past conically cambered slender delta wings with leading-edge separation." ARC R & M 3748 (1972)

44 E.S. Levinsky, H.H.Y. Wei: "Non-linear lift and pressure distribution on slender conical bodies with strakes at low speeds." NASA CR-1202 (1968)

45 C. Rehbach: "Étude numérique de nappes tourbillonnaires issues d'une ligne de décollement près du bord d'attaque." Rech. Aero., No.6, 325-30 (1973)

46 W. Schröder: "Berechnung der nichtlinearen Beiwerte von Flügeln mit kleinem und mittlerem Seitenverhältnis nach dem Wirbelleiterverfahren in inkompressibler Strömung." DFVLR-78-26 (1978); Trans. as ESA-TT-585

47 S.A. Jepps: "The computation of vortex flows by panel methods." VKI Lecture Series 5, Computational Fluid Dynamics (1978)

48 S.M. Belotserkovskii, M.I. Nisht: "Unsteady nonlinear theory for a thin wing of arbitrary planform." Izv. Ak. Nauk Mekh. Zh. Gaza, No.4, 100-8 (1974); Trans. in Fluid Dynamics, 9, 583-9

49 E.H. Atta, O.A. Kandil, D.T. Mook, A.H. Nayfeh: "Unsteady aerodynamic loads on arbitrary wings including wing-tip and leading-edge separation." AIAA Paper 77-156 (1977)

50 O.A. Kandil, E.H. Atta, A.H. Nayfeh: "Three-dimensional steady and unsteady asymmetric flow past wings of arbitrary planforms." NASA CR-145235 (1977)

51 V.A. Aparimov, S.M. Belotserkovskii, M.I. Nisht, O.N. Sokolova: "On the mathematical simulation in an ideal fluid of separated flow past a wing and the destruction of the vortex sheet." Dokl. Ak. Nauk SSSR, 227, 820-3 (1976); Trans. in Sov. Phys. Dokl., 21, 4, 181-3

52 C. Rehbach: "Calcul numérique d'écoulement tridimensionels instationnaires avec nappes tourbillonnaires." Rech. Aero. 1977-5, 289-98 (1977)

53 C. Rehbach: "Calcul instationnaire de nappes tourbillonnaires émises par des surfaces portantes fortement inclinées." Paper 14 in 'High angle of attack aerodynamics', AGARD CP 247 (1978)

54 M.G. Hall: "A numerical method for solving the equations for a vortex core." RAE Technical Report 65106 (1965)

55 A. Rizzi: "Numerical solution of Euler equations simulation of three-dimensional vortex flow." In AGARD FDP Symposium 'Aerodynamics of vortical type flow in three dimensions' (1983)

56 M.J. Lighthill: "Mathematics in aeronautics." J. Roy. Aeron. Soc. 64, 375-84 (1960)

57 D. Küchemann: "The aerodynamic design of aircraft." page 513, Pergamon (1978)

58 J.H.B. Smith: "A review of separation in steady three-dimensional flow." Paper 31 in 'Flow separation', AGARD CP 168 (1975)

59 B.L. Hunt: "Asymmetric vortex forces and wakes on slender bodies." AIAA Paper 82-1336 (1982)

60 E.R. Keener, G.T. Chapman, L. Cohen, J.T. Taleghani: "Side-forces on forebodies at high angles of attack and Mach numbers from 0.1 to 0.7; two tangent ogives, paraboloid and cone." NASA TM X-3438 (1977)

61 I.P. Jones: "Flow separation from yawed delta wings." Computers & Fluids 3, 155-77 (1975)

62 D.J. Peake, F.K. Owen, D.A. Johnson: "Control of forebody vortex orientation to alleviate side-forces." AIAA Paper 80-0183 (1980)

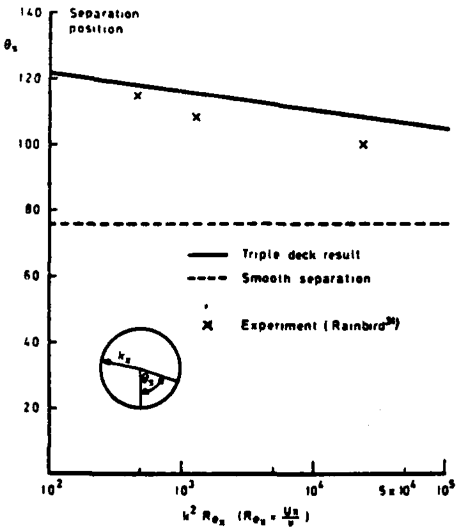

Fig 1 Variation of laminar separation position on a circular cone with a scaled Reynolds number (Fiddes[25])

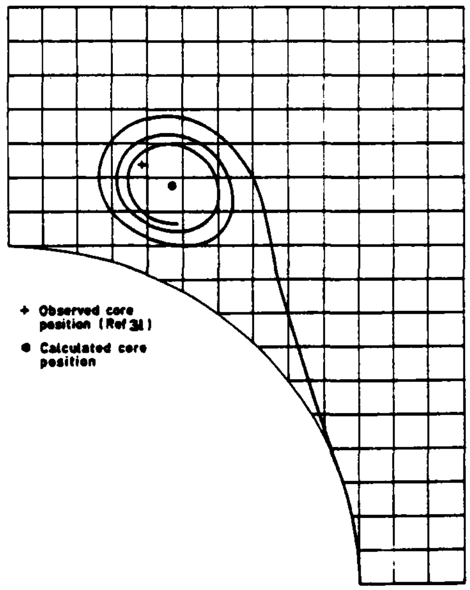

Fig 2 Observed core position on a circular cone compared with vortex-sheet calculation for same, laminar, separation position (Fiddes[25])

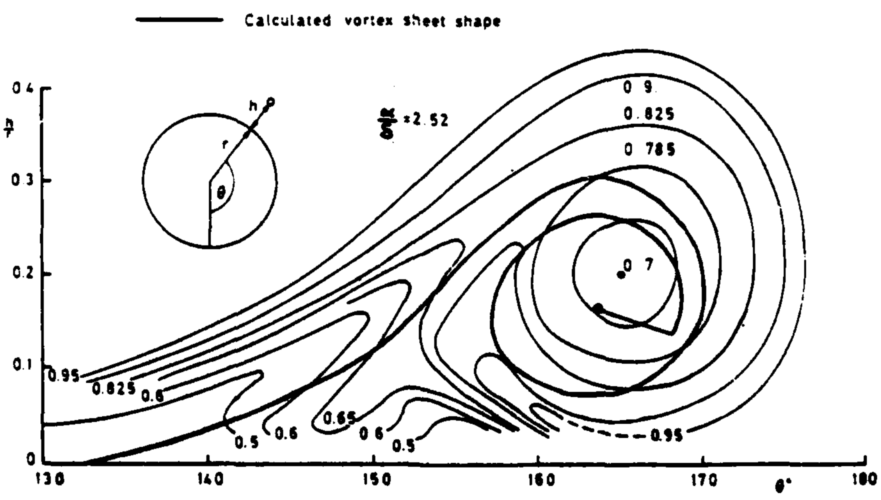

Fig 3 Observed contours of total pressure on circular cone[32] compared with vortex sheet calculation for same, turbulent, separation position (Fiddes[25])

Figs 4-7

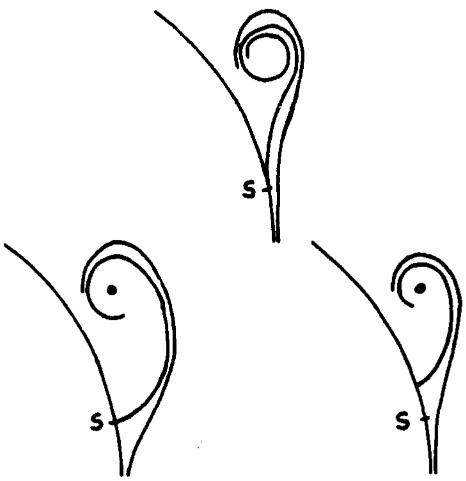

Fig 4 Effect of different Kutta conditions on conical streamline patterns (sketch only)

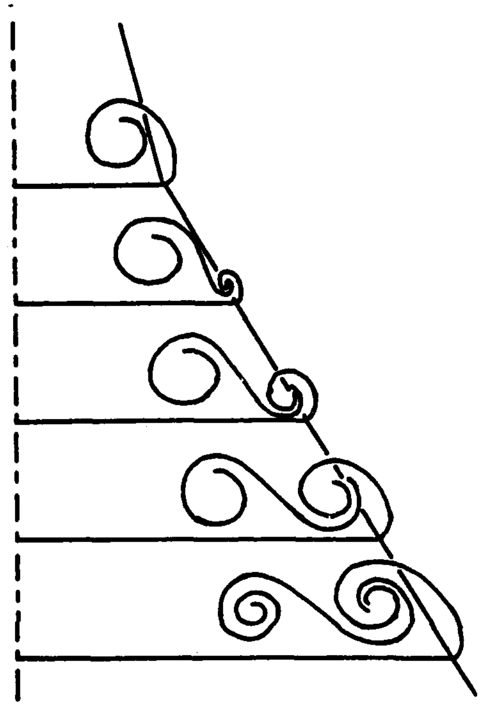

Fig 5 Shape of vortex sheet on double-delta wing with small change in sweep-back angle (sketch)

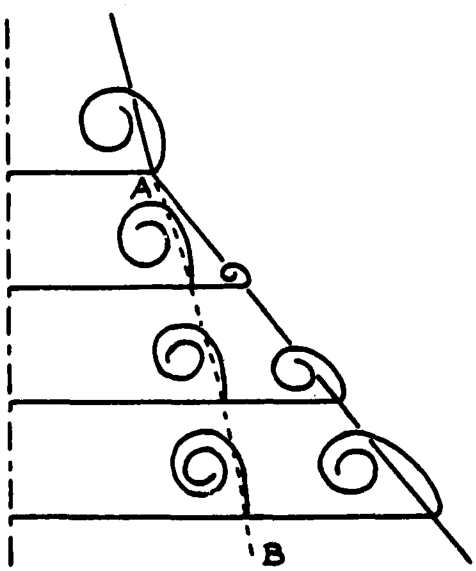

Fig 6 Shape of vortex sheet on double-delta wing with moderate change in sweep-back angle (sketch)

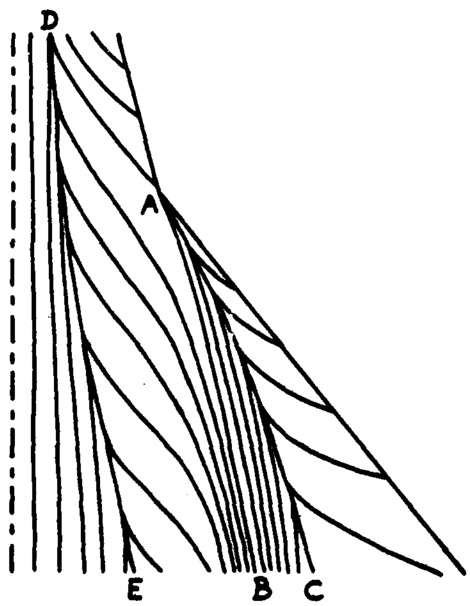

Fig 7 Surface streamline pattern on double-delta wing with moderate change in sweep-back angle (sketch)

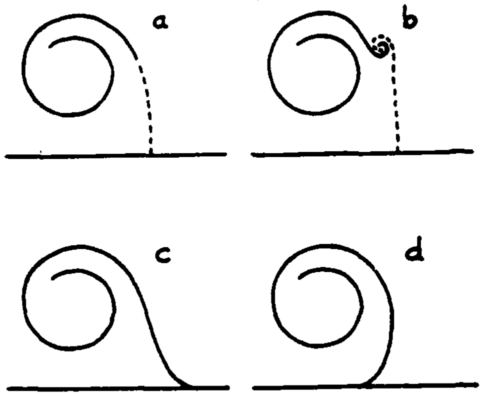

Fig 8 Possible forms for inboard vortex sheet (——) and stream surface (-----) (sketch)

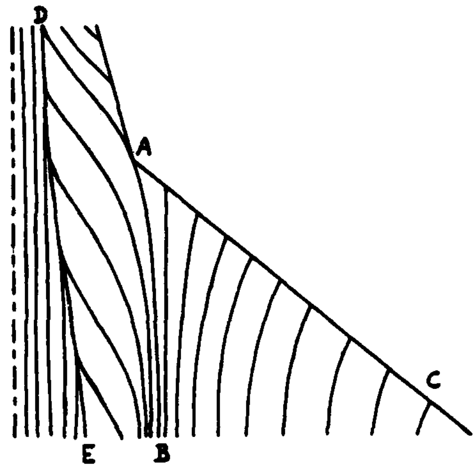

Fig 9 Surface streamline pattern on double-delta wing with attached flow on outboard panel (sketch)

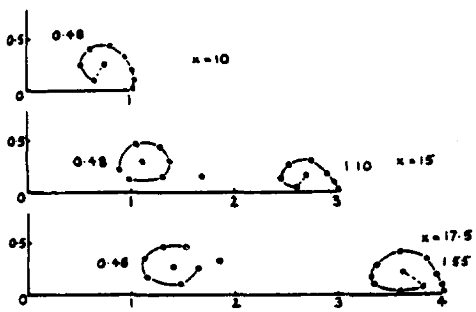

Fig 10 Calculated vortex configuration on double-delta wing at low incidence (Peace[24])

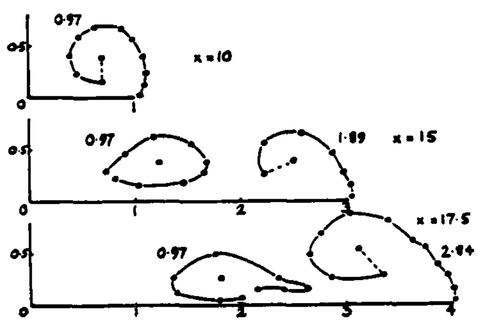

Fig 11 Calculated vortex configuration on double-delta wing at higher incidence (Peace[24])

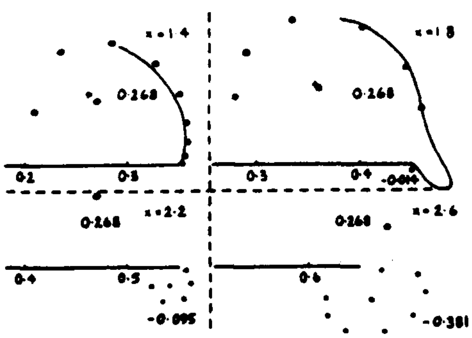

Fig 12 Calculated vortex configuration on delta wing with lengthwise camber (——, + Clark[9]; o,• Peace[24])

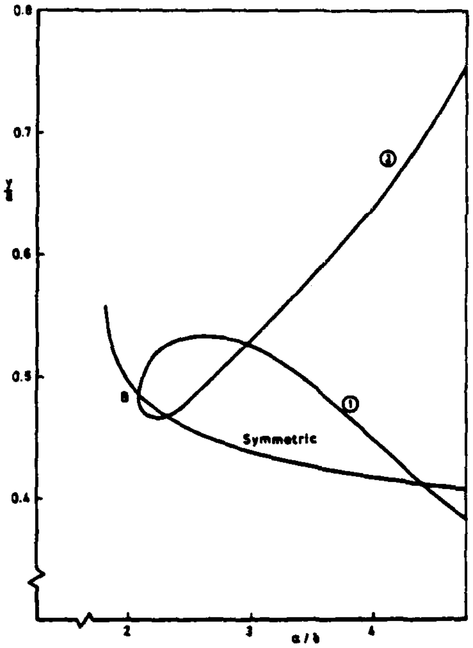

Fig 13a Bifurcation of line-vortex solutions for circular cone[40]
(a) lateral position of vortices

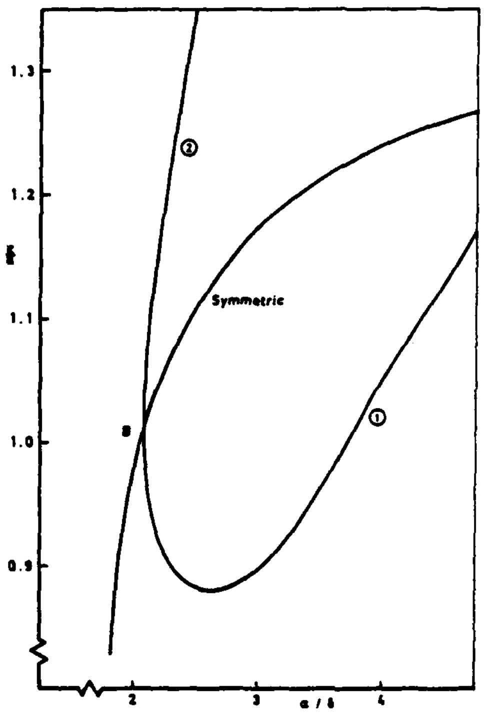

Fig 13b Bifurcation of line-vortex solutions for circular cone[40]

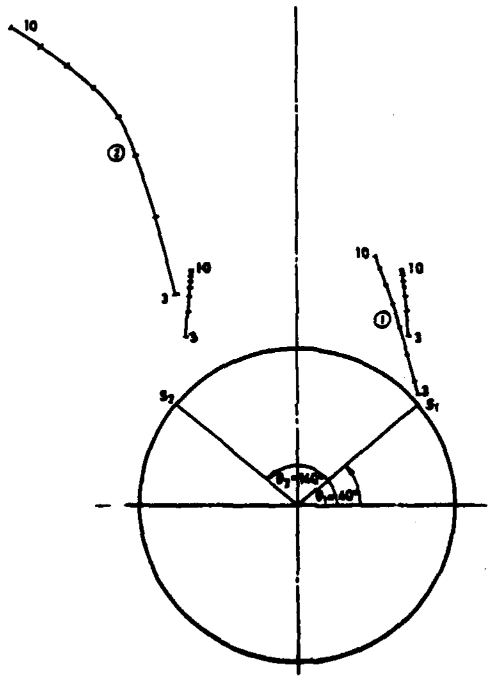

Fig 14 Variation with incidence parameter of vortex positions for symmetric separation lines on circular cone[40]

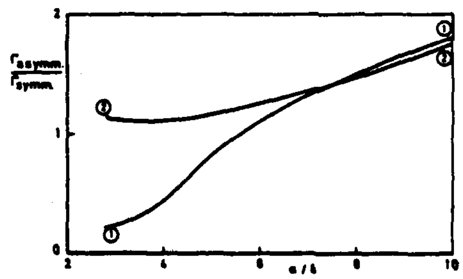

Fig 15 Circulations of asymmetric vortices referred to symmetric values for circular cone[40]

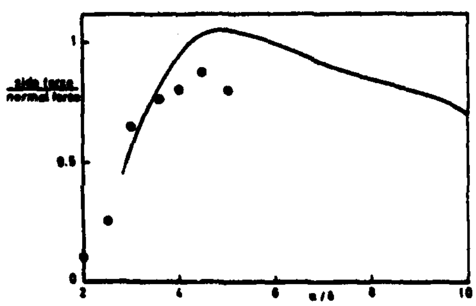

Fig 16 Ratio of side to normal force on circular cone; theory[40] and measurement[60]

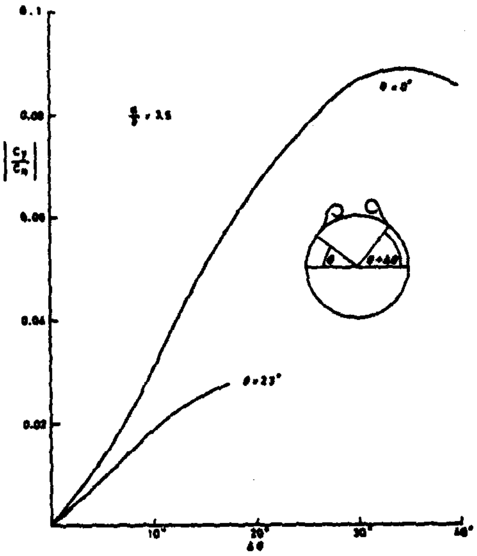

Fig 17 Effect on side force of asymmetry in separation line position for first family of line-vortex solutions[28]

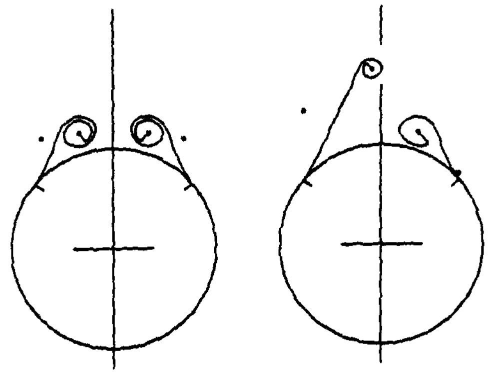

Fig 18 Symmetric and asymmetric solutions with symmetric separation lines; vortex sheet[28] and line-vortex[40] solutions

(b) $\alpha/\theta_c = 3.2$

Fig 19 Shadowgraph of vortex configuration on circular cone, from behind the base (Peake, *et al*[62])

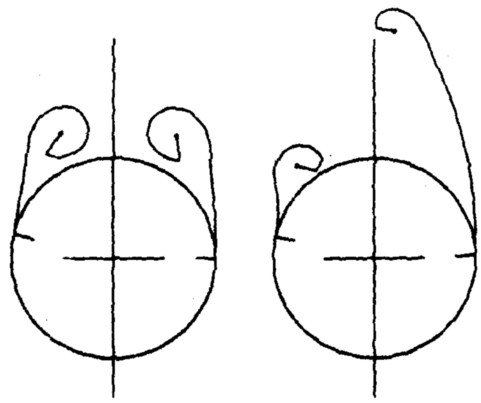

Fig 20 First (left) and second (right) family solutions for observed, laminar, separation lines[28]

END

DATE

FILMED

12 83